Size Dependence of Exchange Bias in Co/CoO Nanostructures

Sara Laureti,[1,2] Sarah Y. Suck,[2] Helge Haas,[2] Eric Prestat,[3] Olivier Bourgeois,[2] and Dominique Givord[2]

[1]*ISM-CNR, Area della Ricerca Roma1, Via Salaria km 29.300, Monterotondo Scalo, Roma, Italy*
[2]*Institut NÉEL, CNRS-UJF, 25 rue des Martyrs, 38042 Grenoble, France*
[3]*CEA-INAC/UJF-Grenoble1 UMR-E, SP2M, LEMMA, Minatec Grenoble, F-38054, France*

(Received 7 July 2011; published 15 February 2012)

In Co/CoO nanostructures, of dimensions $l \times 3l$, at small Co thickness (≈ 6, 10 nm), a strong increase in the bias field and the associated coercive field are found as the nanostructure size is reduced from $l = 120$ nm to $l = 30$ nm. This property indicates that the characteristic length D_{AF} within the antiferromagnet which governs exchange-bias effects is the nanostructure size. By contrast, at larger Co thickness (≈ 23 nm), the exchange-bias field does not depend on the nanostructure size, implying that D_{AF} is smaller than the nanostructure size. The results are discussed in the framework of the Malozemoff model, taking into account that the coupling between CoO grains is weak. Exchange bias is dominated either by coupling within the antiferromagnetic layer (6- and 10-nm-thick Co samples) or by ferromagnetic-antiferromagnetic interfacial coupling (23-nm-thick Co sample).

DOI: 10.1103/PhysRevLett.108.077205 PACS numbers: 75.75.−c, 75.70.Cn

Exchange bias (EB) occurs when a ferromagnet (F) and an antiferromagnet (AF) are coupled by interfacial exchange interactions [1–3]. This phenomenon manifests itself as a shift of the ferromagnetic hysteresis cycle along the field axis. This shift, measured by the exchange-bias field H_{eb}, appears after cooling the EB system under a magnetic field from above a certain temperature, characteristic of some of the antiferromagnet properties. Concomitantly, an increase in the F coercive field occurs.

The EB interfacial coupling effect can be described by the phenomenological equation [2]

$$\gamma A = \mu_0 M_s V H_{eb}, \tag{1}$$

where γ is the interfacial exchange coupling, A is the interfacial surface area, M_s is the spontaneous magnetization of the ferromagnetic layer, and V is the ferromagnetic volume involved.

EB is exploited to pin one of the magnetic layers involved in spin-valve structures. Since the size of the sensitive part of such a spin valve is continuously reduced to meet the requirement of high density recording, the size dependence of exchange-bias phenomena needs to be understood. Most generally, EB models predict that the strength of the exchange-bias field depends on the ratio between some characteristic length D_{AF} over which the uncompensated AF moment and the sample dimensions are defined. Experimentally, the properties of Co/CoO nanostructures, the archetype of the EB systems, were examined in Refs. [4,5]. For square nanostructures, above 200-nm size, it was found that the bias field and the coercive field tend to increase with decreasing size. In other systems, no clear dependence of H_{eb} and H_c on dot size could be established, and it was suggested that this was related to a competition between the increased intrinsic coupling energy and reduced blocking temperature in nanostructures [6]. In this Letter, we report on Co/CoO nanostructures at substantially smaller sizes than in previous studies. As confirmed by magnetic force microscopy (MFM) analysis [7], the nanostructures are essentially in the single-domain state, and their rectangular shape guarantees that a unique magnetization direction is defined. Nanostructure patterning was realized by electron-beam lithography on a resist-coated substrate (standard Si wafers), followed by chemical developing. On the thus-obtained patterned surface, a cobalt layer was deposited by electron gun evaporation using a mechanical mask which permitted that the deposition of the magnetic material be restricted to the patterned area only. For the purpose of the analysis (see below), two series of samples were prepared. The first series contained a CoO layer on the top of the Co layer. The formation of the CoO layer was obtained by exposing the freshly deposited Co layer to a pure oxygen atmosphere at a pressure of 10^{-2} mbar during 5 minutes. The thickness of the CoO layer was about $t_{CoO} = 3$ nm, as derived from magnetization measurements, x-ray photoelectron spectroscopy depth-profile analysis, and TEM line scan [8], corresponding to 2 nm of metallic Co being oxidized. For the samples of the second series, the oxidation stage was not applied. The samples from both series were coated with a 7-nm Au film, protecting them against further oxidation. Finally, a lift-off procedure was applied to free the nanostructures.

The complete patterned arrays covering a surface area of about 4 mm^2 contained typically 10^7–10^8 nanostructures. Samples of 3 categories were prepared, each being characterized by the nanostructure's lateral size: (i) small nanostructures (samples S) (with dimension 30×90 nm^2), (ii) medium nanostructures (samples M) (60×180 nm^2), and (iii) large nanostructures (samples L) (120×360 nm^2), respectively. For each category, samples with

three different Co thicknesses were deposited: $t_{Co} = 8$, 12, and 25 nm, respectively. In the following, the Co thickness for a given sample is indicated as a lower index attached to the letter S, M, or L (samples submitted to the oxidation stage) or S', M', or L' (samples not submitted to the oxidation stage). For the purpose of comparison, an unpatterned 25-nm-thick continuous film was prepared, as well.

The periodicity of the nanostructure array was $2l$ along the x axis and $3l$ along the y axis (see left-hand side of Fig. 1), l being the width of the nanostructure. Under these conditions, the dipolar field created on a given nanostructure by the neighboring ones was calculated to be less than 3 mT, whatever the system magnetization state. A MFM analysis confirmed that magnetization reversal was not significantly influenced by dipolar interactions [7].

The magnetic characterization was carried out using a superconducting quantum interference device magnetometer in a maximum applied field of 5 T, between 4 and 300 K. Before each measurement, the sample was field cooled from 300 K under an in-plane magnetic field of 1 T and applied along the y axis, i.e., parallel to the nanostructure's long dimension. The directions of the cooling field and that of the measuring field were always the same. The measurements started from low temperature and extended to above the blocking temperature T_B. The measured hysteresis loops were corrected by subtracting the substrate's diamagnetic background (see Fig. 2). H_{eb} and H_c were derived at each temperature from the values of the switching fields under negative and positive applied magnetic fields, respectively. These switching fields were defined as the fields at which the derivative of the magnetization variation is maximum. Note that H_{eb} and H_c were extracted from the trained loop [2].

Let us discuss first the properties of the Co/Au nanostructures (see Table I) not submitted to the oxidation stage. In the three M' samples (M'_8, M'_{12}, and M'_{25}), exchange-biased cycles were found below a blocking temperature of about 50 K. Within experimental accuracy, the bias field has the same value in all 3 samples, equal to $\mu_0 H_{eb} \approx 10$ mT at 4 K. In sample S'_8, the 4-K bias field amounts to 17 mT, and, in the large sample L'_{25}, it amounts to 4 mT only. As illustrated in Fig. 1(b), exchange bias in these Co/Au nanostructures is due to the CoO formed on the nanostructure's unprotected side [see the illustration in Fig. 1(b)]. Thus, the surface area A' [A in Eq. (1)] is equal to $(8l - 8t_{CoO})t_{Co}$, where t_{Co} is the Co thickness, $M_S = M_{Co}$ is the Co metal spontaneous magnetization, $V' = (l - 2t_{CoO})(3l - 2t_{CoO})t_{Co}$ is the associated Co volume, and H'_{eb} is the associated exchange-bias field. Expression (1) predicts then that the bias field H'_{eb} is independent of t_{Co}, as observed experimentally for samples M' (see Table I), and proportional to $A/M_S V$, as revealed by comparing all samples of this category. The derived interfacial exchange energy is $\gamma' = 0.3$ mJ/m^2.

Consider now the Co/CoO/Au nanostructures. The low-temperature hysteresis cycles of samples S_{25}, M_{25}, and L_{25} are shown in Fig. 2, and the temperature dependence of the bias field in all samples is shown in Fig. 3. In general, H_{eb} is very significantly increased with respect to the corresponding field in a continuous film ($\mu_0 H_{eb} = 25$ mT at 4 K for the 25-nm-thick continuous film). Furthermore, both H_{eb} and H_c (not shown) increase as the nanostructure's size is decreased. The exchange-bias field vanishes at about 140 K.

EB in these Co/CoO/Au nanostructures is due to two contributions: (i) a contribution from CoO formed on the side of the Co nanostructures, as in the Co/Au nanostructures, and (ii) a contribution from CoO formed on the top of the nanostructures during the oxidation process. The EB values are much larger in Co/CoO/Au than in Co/Au, which implies that the CoO top-layer contribution is dominant. In view of discussing quantitatively the top-layer contribution to H_{eb}, the side-layer contribution, assumed

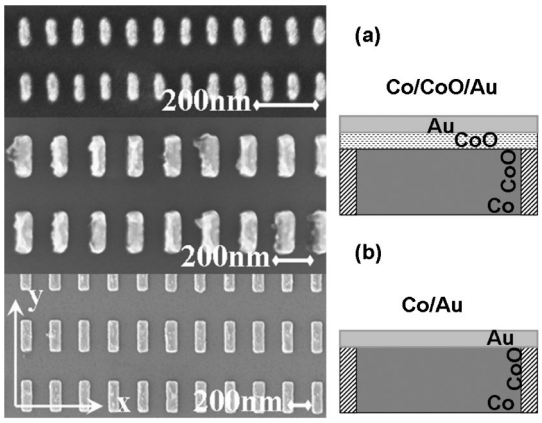

FIG. 1. Left: Scanning electron microscope images of S_{25}, M_{25}, and L_{25} samples (from top to bottom). Right: Side-view scheme of (a) Co/CoO/Au and (b) Co/Au nanostructures, illustrating the oxidation of the Co top and side surfaces.

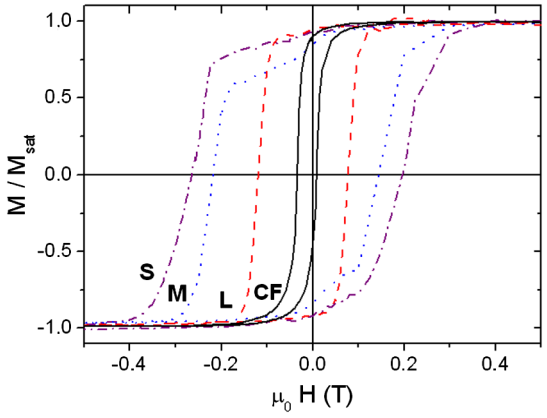

FIG. 2 (color online). M-H loops revealing the reversal of S_{25}, M_{25}, and L_{25} nanostructures, compared to the one of a continuous film (CF). All loops are measured at 4 K. Note that the magnetization M is normalized to the saturated magnetization M_{sat}.

TABLE I. Exchange-bias field ($\mu_0 H_{eb}$) and coercive field ($\mu_0 H_c$) at 4 K for samples S', M', and L' (Co/Au nanostructures) and samples S, M, and L (Co/CoO/Au nanostructures). The given Co thicknesses are nominal thicknesses. The top-layer contribution to the bias field ($\mu_0 H_{eb}^{top}$) and to the coercive field ($\mu_0 H_{c(eb)}^{top}$) were obtained by subtracting the bias field $\mu_0 H'_{eb}$ or the coercive field $\mu_0 H'_c$ in samples S', M', and L' from the corresponding field in samples S, M, and L. The values between parentheses for samples S', M', and L' were not measured directly but derived from values measured in other samples (see text).

t_{Co} (nm)		8			12			25	
H(mT)	S'/S	M'/M	L'/L	S'/S	M'/M	L'/L	S'/S	M'/M	L'/L
$\mu_0 H'_{eb}$	17	11	(4)	(17)	9	(4)	(17)	10	4
$\mu_0 H'_c$	256	111	(68)	(256)	118	(68)	(256)	140	68
$\mu_0 H_{eb}$	236	174	90	151	119	50	41	31	30
$\mu_0 H_c$	449	286	156	450	261	105	261	267	104
$\mu_0 H_{eb}^{top}$	219	163	86	134	110	46	24	21	26
$\mu_0 H_{c(eb)}^{top}$	193	175	88	194	143	37	4	127	36

to be equal to H'_{eb} in Co/Au nanostructures, was subtracted from the experimental H_{eb} of the Co/CoO/Au nanostructures; the H_{eb}^{top} values thus obtained are gathered in Table I.

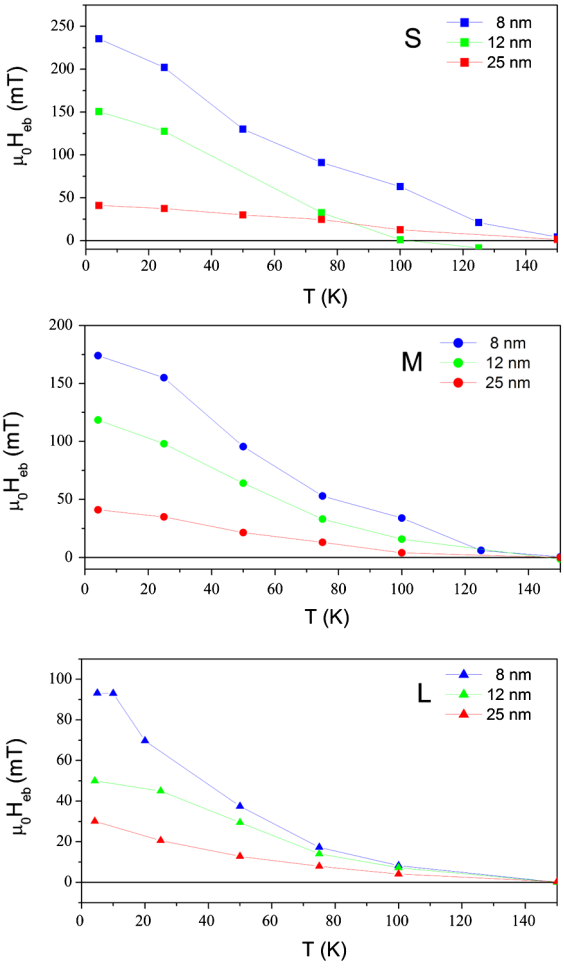

FIG. 3 (color online). Temperature dependence of $\mu_0 H_{eb}$ in Co/CoO/Au samples measured for the three nanostructure sizes S (squares), M (dots), and L (triangles).

For the 3 samples (S, M, and L) with the thickest Co layer ($t_{Co} = 25$ nm), H_{eb}^{top} is approximately equal to 25 mT, the bias field found in the corresponding continuous Co/CoO films being independent of the nanostructure size. Further, as shown by Fig. 4, in L samples, H_{eb}^{top} varies approximately linearly, with $A/M_S V$ equal to $1/M_S(t_{Co} - t_{CoO})$. The value of γ_L that is derived, 0.8 mJ/m^2, is 3 times larger than the Co/CoO interfacial energy determined on the nanostructure sides. Consistent with the higher value of the exchange coupling constant, exchange bias develops at higher temperature (140 K) than the 50 K found in the Co/Au nanostructures.

The difference between the interfacial exchange energy on the nanostructure side surface, as compared to the nanostructure top surface, may be related to the fact that side oxidation occurs *ex situ* in air whereas top-surface oxidation takes place *in situ* under 10^{-2} mbar of a pure

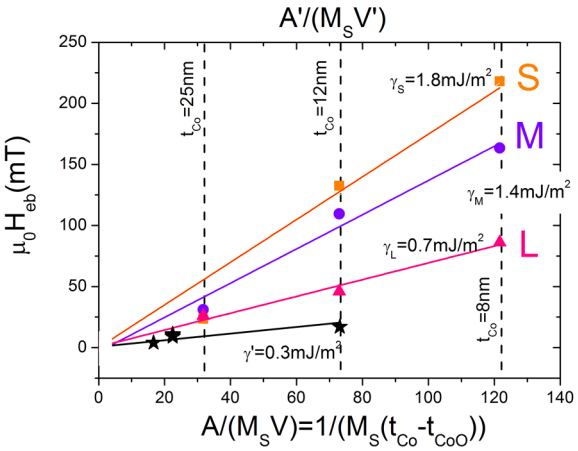

FIG. 4 (color online). $\mu_0 H_{eb}$ as a function of $A/M_s V$ for the samples S (orange squares), M (purple dots), and L (pink triangles) for all the thicknesses. The black stars show the $\mu_0 H_{eb}$ for the Co/Au samples. The linear fits give the values of γ for each of the geometries.

oxygen atmosphere. Several experimental data already revealed that the strength of the exchange coupling in Co/CoO depends strongly on the oxidation procedure used for the formation of the oxide layer [2]. An additional feature emerges from these data. As one goes from the 25-nm-thick sample to the 12- and 8-nm-thick samples, H_{eb}^{top} is found to become dependent on the nanostructure size and is actually enhanced at small dimensions (Fig. 4). The exchange coupling constants (γ_M and γ_S) extracted from this graph amount to 1.4 mJ/m^2 and 1.8 mJ/m^2, respectively.

Assuming a continuous antiferromagnetic single crystalline layer, Malozemoff [9] has shown that the exchange field due to the F layer acts as a random field on the AF one. Consequently, correlated regions form in the antiferromagnet with characteristic dimension D_{AF}. In the case of polycrystalline films, several studies have assumed that the AF grains are essentially exchange-decoupled [10,11]. However, in the same way as the F-AF coupling at the origin of exchange bias is due to incomplete compensation, it is likely that some frustrated coupling persists between AF grains. In the particular case of CoO, the existence of this coupling is experimentally revealed by the fact that the blocking temperature of an assembly of core-shell Co/CoO grains dispersed on a surface increases drastically when the grain shells come into contact [12]. Consistently, in the following discussion, we consider both $e_{F\text{-}AF}$, the F-AF exchange coupling energy per unit surface area between an antiferromagnetic grain and the ferromagnetic layer, and $e_{AF\text{-}AF}$, the exchange coupling energy per unit surface area of an antiferromagnetic domain wall. This analysis is not in contradiction with models assuming exchange decoupling between AF grains, in the sense that $e_{AF\text{-}AF}$ is much smaller than the exchange energy between two moments within a given CoO grain. The total coupling energy, E_T, writes per interfacial unit surface area

$$E_T = \frac{1}{D_{AF}}(2t_{CoO}e_{AF\text{-}AF} - 2r_g e_{F\text{-}AF}), \qquad (2)$$

where r_g is the radius of the AF grains and D_{AF} the correlation length resulting from the coupling. Equation (2) is similar to Eq. (3) in [9] with the AF domains being taken as simple cylinders, as justified by the very small thickness of the CoO layer and by the fact that CoO ultrathin films present columnar structure [13].

D_{AF} in Eq. (2) will self-adjust in order to minimize the energy E_T. The two terms $e_{F\text{-}AF}$ and $e_{AF\text{-}AF}$ are essentially unknown. Assuming that the first term of the right-hand side, representing antiferromagnetic intergrain coupling, dominates, D_{AF} should go to infinity (as noted by Malozemoff, additional small energy terms will in this case define ultimately the domain size [9]). However, in the present case, D_{AF} is bounded by the nanostructure size l, and this provides a mechanism by which E_T (and γ) may become nanostructure-size-dependent [6]. The bias field is expected to vary as $1/l$, increasing by a factor of 4 from L to S nanostructures, in qualitative agreement with the experimental results for Co 8-nm and Co 12-nm nanostructures.

Assume reciprocally that the F-AF coupling in Eq. (2) dominates AF-AF coupling. D_{AF}, in this case, will tend to its smallest possible value, which is the AF grain size. In this case, the H_{eb}^{top} bias field becomes independent of the nanostructure size. This situation accounts for the behavior found in the 25-nm-thick Co nanostructures. Consistently, the bias field for such 25-nm-thick samples is close to the value found in continuous films. Note that, from Eq. (2), one may be tempted to conclude that the bias field at small D_{AF} should be large, which is unlike the experimental observation. Actually, only the AF grains of which magnetization is frozen during the F-moment rotation contribute to exchange bias. Small D_{AF} implies that a large fraction of AF grains follows the F-moment rotation, which in turn tends to lower the bias field value.

Altogether, these results indicate that, at small Co thickness, the value of D_{AF} is of the order of l, whereas, at large Co thickness, it is smaller than l. In view of understanding this difference, an 8-nm-thick Co/CoO/Au sample was prepared, following the same procedure as for the preparation of the various other samples, and a slice, approximately 50 nm thick, was cut by a focused ion beam. TEM observations and electron energy-loss spectroscopy line scans (see Supplemental Material [8]) revealed that the Co films have a granular stucture. From dark-field and bright-field images, the size of the Co grains is deduced to be approximately 8 nm, significantly smaller than the nanostructure sizes even for samples S. Such a microstructure implies that the thickness of the Co film varies from point to point, in particular, being reduced in the regions between the grains. In the thinnest samples, a complete separation or a partial separation between the Co grains may happen, favored by oxidation. This phenomenon provides a simple explanation for the relative reduction of $e_{F\text{-}AF}$ in the thinnest samples compared to the 25 nm samples.

It should be noted that, in case $e_{F\text{-}AF}$ and $e_{AF\text{-}AF}$ have approximately the same value, crossing between the two terms in Eq. (2) may result from a minor change of one of them and provoke a dramatic modification of the correlation length from infinity, thus limited to the nanostructure size, to zero and limited to the AF grain size.

The coercive field is the second important parameter of exchange-bias systems. A larger coercive field is found in the Co/CoO/Au nanostructures than in the Co/Au ones, which directly reveals the influence of interfacial exchange coupling on coercivity. In order to extract the coercive field H_c^{top} associated to the exchange-bias field H_{eb}^{top}, the experimental coercive field measured on the Co/Au samples was systematically subtracted from the H_c measured in the Co/CoO/Au. In the case where a Co/Au sample had not

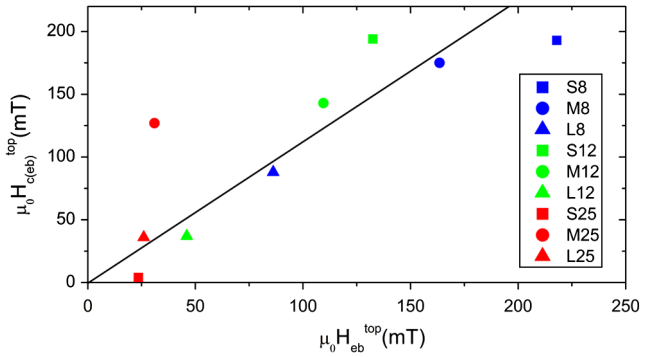

FIG. 5 (color online). $H_{c(eb)}^{top}$ as a function of H_{eb}^{top} for all the sample thicknesses for the S, M, and L geometries. The linear fit gives a proportionality of 1 between both axes.

been prepared corresponding to a Co/CoO/Au one (see Table I), the coercive field of the Co/Au was assumed to be equal to that of another sample of different size but same Co thickness. This is in agreement with the fact that the coercive field of M' samples is independent of the Co thickness (see Fig. 4). Beyond the generally accepted fact that the bias field and the coercive field are linked, the data in Fig. 5 reveal that H_c^{top} is approximately proportional to H_{eb}^{top}. In all cases, H_c^{top} here measured is due to the rotation of some AF entities above their anisotropy barrier under the action of exchange coupling. The larger γ is, the larger the fraction of AF grains which follow the rotation of the F grains. In case the distribution of the energy barrier is flat, this additional fraction is proportional to γ, and thus to exchange bias, hence giving an account for the observed behavior.

In summary, in the Co-thin Co/CoO nanostructures ($t_{Co} = 8$ and 12 nm), the characteristic dimension D_{AF} which governs exchange bias is equal to the nanostructure size l. By contrast, in 25-nm-thick Co nanostructures, the bias field is not dependent on the nanostructure size and it is equal to the bias field found in continuous films. This implies that $D_{AF} < l$. The larger value of D_{AF} in Co-thin nanostructures is tentatively attributed to the fact that the Co layer becomes discontinuous upon oxidation.

We thank T. Fournier and the technical staff of Nanofab for their support in the nanofabrication, as well as the microscopy network METSA and Dr. P. Bayle-Guillemaud for her support during the TEM observations, and finally Dr. Yuepeng Zhang for fruitful discussions concerning the links between magnetic and nanostructural properties in EB systems.

[1] W. H. Meiklejohn and C. P. Bean, Phys. Rev. **102**, 1413 (1956).
[2] J. Nogués and I. K. Schuller, J. Magn. Magn. Mater. **192**, 203 (1999).
[3] J. Nogués, J. Sort, V. Langlais, V. Skumryev, S. Suriñach, J. S. Muñoz, and M. D. Baró, Phys. Rep. **422**, 65 (2005).
[4] E. Girgis *et al.*, Phys. Rev. Lett. **91**, 187202 (2003).
[5] K. Temst *et al.*, Eur. Phys. J. B **45**, 261 (2005).
[6] V. Baltz, J. Sort, S. Landis, B. Rodmacq, and B. Dieny, Phys. Rev. Lett. **94**, 117201 (2005).
[7] S. Y. Suck, U. Wolff, V. Neu, S. Bahr, O. Bourgeois, and D. Givord, Appl. Phys. Lett. **95**, 162503 (2009).
[8] See Supplemental Material at http://link.aps.org/supplemental/10.1103/PhysRevLett.108.077205 for a TEM and electron energy-loss spectroscopy detailed study of the Co/CoO/Au layers.
[9] A. P. Malozemoff, Phys. Rev. B **35**, 3679 (1987).
[10] E. Fulcomer and S. H. Charap, J. Appl. Phys. **43**, 4190 (1972).
[11] K. O'Grady, L. E. Fernandez-Outon, and G. Vallejo-Fernandez, J. Magn. Magn. Mater. **322**, 883 (2010).
[12] J. Nogués, V. Skumryev, J. Sort, S. Stoyanov, and D. Givord, Phys. Rev. Lett. **97**, 157203 (2006).
[13] M. Molina-Ruiz, A. F Lopeandia, F. Pi, D. Givord, O. Bourgeois, and J. Rodriguez-Viejo, Phys. Rev. B **83**, 140407 (2011).